European Journal of Pharmaceutics and Biopharmaceutics 70 (2008) 615–620

Contents lists available at ScienceDirect

European Journal of Pharmaceutics and Biopharmaceutics

journal homepage: www.elsevier.com/locate/ejpb

Research paper

Reversible lipidization of somatostatin analogues for the liver targeting

Liyun Yuan [a], Jeff Wang [b], Wei-Chiang Shen [a,*]

[a] Department of Pharmacology and Pharmaceutical Sciences, University of Southern California, Los Angeles, USA
[b] Department of Pharmaceutical Sciences, Western University of Health Sciences, Pomona, USA

ARTICLE INFO

Article history:
Received 21 August 2007
Accepted in revised form 5 May 2008
Available online 17 May 2008

Keywords:
Tyr^3-octreotide
Reversible lipidization
Liver targeting
Parenchymal cells
Nonparenchymal cells
Hepatocellular carcinoma

ABSTRACT

Tyr^3-octreotide (TOC), a somatostatin analogue, is reversibly lipidized for passive delivery to the liver with the aim of increasing its association with hepatocytes. The reversibly lipidized TOC (REAL-TOC) was formed by the conjugation of the *N*-palmitoyl cysteinyl moiety to the cysteinyl residues of reduced TOC through disulfide linkages and characterized by matrix-assisted laser desorption/ionization (MALDI)-time of flight (TOF) analysis. The measured mass of REAL-TOC $(M+H)^+$ is 1752.31 Da (calculated mass: 1752.78), confirming that two molecules of *N*-palmitoyl cysteines are linked to TOC via disulfide bonds. TOC and REAL-TOC were radioiodinated and administered to mice. Their biodistribution and intrahepatic distribution were subsequently investigated. The area under the curve (AUC) of ^{125}I-REAL-TOC in the liver was 3.8-fold greater than that of ^{125}I-TOC, with 20.5% and 5.8% of the injected dose (ID)/g of ^{125}I-REAL-TOC remaining in the liver at 2 and 24 h post injection, respectively. Within the liver, TOC was primarily distributed to parenchymal cells (PC). Nevertheless, TOC was quickly excreted out and only 2.4% ID per 100 mg protein remained in the PC at 2 h post injection. ^{125}I-REAL-TOC was retained in PC for up to 2 h with a constant concentration of around 6% ID/100 mg protein. ^{125}I-REAL-TOC was also highly associated with nonparenchymal cells (NPC) at significantly higher levels than ^{125}I-TOC at 10 min, 1 h and 2 h post injection. Since somatostatin analogues have been evaluated for treating late-stage hepatocellular carcinoma (HCC), the reversibly lipidized conjugates may possess enhanced therapeutic efficacy due to the liver-targeting effect.

1. Introduction

Many liver diseases such as chronic viral hepatitis, liver fibrosis and hepatocellular carcinoma require long-term drug therapy. Delivery of drugs specific to the liver will decrease side effects by reducing drug distribution in nontarget cells and improve the therapeutic efficacy by concomitantly increasing the drug concentration in target cells. Sugar moieties are commonly used to modify drugs for the selective targeting to asialoglycoprotein receptors in hepatocytes and mannose receptors in Kupffer and liver endothelial cells [1–3]. However, binding to carbohydrate receptors will trigger the internalization of the conjugated drugs, and the intracellular degradation is often favored over the release of drugs in the endocytotic pathway [4]. This targeting strategy is especially less favorable for peptide and protein drugs that act on cell surface receptors to activate downstream signaling pathways, such as somatostatin analogues and interferons [5–7].

To overcome these drawbacks in liver targeting, we have taken the lipidization approach to modify protein and peptide drugs for passive liver targeting, aiming at enhancing the association of this type of drugs with liver cell membranes. In this report, we describe the application of reversible aqueous lipidization (REAL) technology [8–10] to conjugate the palmitoyl acid to cysteinyl residues of a somatostatin analogue, Tyr^3-octreotide (TOC) via reversible disulfide linkages. Somatostatin analogues such as octreotide have been well established in clinical settings to treat endocrine tumors, and their therapeutic actions are achieved through binding to somatostatin receptors on tumor cells [5]. Long-acting octreotide has currently been under evaluation for treating late-staged hepatocellullar carcinoma (HCC) [11–15]. In our study, the pharmacokinetic profiles and intrahepatic distribution of TOC and lipidized TOC (REAL-TOC) were compared.

2. Materials and methods

2.1. Materials

Tyr^3-octreotide (TOC) (Fig. 1A) was synthesized by Genemed Synthesis, Inc. (San Antonio, TX, USA). BCA protein assay reagent kit was purchased from Pierce Biotechnology (Rockford, IL, USA). Collagenase IV was a generous gift from Dr. Natalia Cohen (University of Southern California, Los Angeles, CA, USA). All other

* Corresponding author. Department of Pharmacology and Pharmaceutical Sciences, School of Pharmacy, University of Southern California, 1985 Zonal Avenue, PSC 404B, Los Angeles, CA 90089, USA. Tel.: +1 3234421902; fax: +1 3234421390.
E-mail address: weishen@usc.edu (W.-C. Shen).

0939-6411/$ - see front matter © 2008 Elsevier B.V. All rights reserved.
doi:10.1016/j.ejpb.2008.05.004

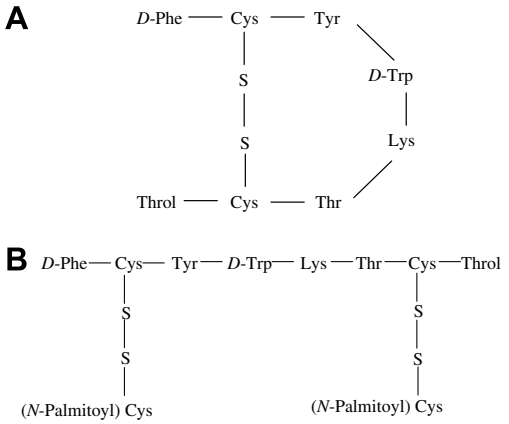

Fig. 1. The structure of TOC (A) and REAL-TOC (B).

chemicals and reagents were obtained from Sigma Chemical Co. (St. Louis, MO, USA).

2.2. Animals

Adult male CF-1 mice aged 6–8 weeks were obtained from Charles River Laboratories (Wilmington, MA, USA) and handled in accordance with the "Principles of Laboratory Animal Care" (NIH 85-23, revised 1985). The animals were allowed a standard diet and tap water *ad libitum*, and were maintained under controlled conditions (12-h light, 12-h dark cycle; 24 °C).

2.3. Preparation of REAL-TOC

TOC structure (Fig. 1A) is modeled from octreotide [16]. REAL-TOC (Fig. 1B) was synthesized as previously described [10]. A solution of 5.0 mg of TOC in 0.9 ml of DMF was mixed with 1.14 mg of dithiothreitol (DTT) in 0.1 ml of DMF at 37 °C for 40 min to reduce the disulfide bond between Cys^2 and Cys^7 of TOC. *N*-Palmitoyl cysteinyl 2-pyridyl disulfide (PAL-CPD, 10.35 mg) was subsequently added to the solution and the reaction mixture was stirred for 30 min at 25 °C. The mixture was diluted with 10 ml of 50 mM ammonium bicarbonate and loaded on a disposable C18 column. The product was eluted from the column with 90–95% methanol. The fractions containing REAL-TOC were pooled, and the solvent was removed by rotary evaporation.

2.4. Characterization of REAL-TOC

The analysis was conducted on an HP1050 HPLC (Hewlett–Packard, Avondale, PA, USA) system with the wavelength set at both 214 nm and 280 nm using a Jupiter C4 column (4.6 × 250 mm; Phenomenex, Torrance, CA, USA). The mobile phase solvents were 10% acetonitrile in 50 mM ammonium bicarbonate, pH 8.0 (A) and 95% acetonitrile in 50 mM ammonium bicarbonate, pH 8.0 (B). A linear gradient from 10% to 100% of B was applied for 20 min at a flow rate of 1 ml/min.

Mass determination using matrix-assisted laser desorption/ionization (MALDI)-time of flight (TOF) analysis was also performed (Proteomic Core Facility, University of Southern California). Approximately 10 pmol of each sample in 10 μl DMF was spotted onto a matrix of 10 mg/ml α-cyano-4-hydroxycinnamic acid in 0.1% trifluoroacetic acid/70% acetonitrile and subjected to MALDI-TOF analysis in an Axima-CFR (Kratos Analytical, Spring Valley, NY) with reflectron mode following calibration.

2.5. Pharmacokinetic studies of TOC and REAL-TOC

TOC and REAL-TOC were iodinated with $Na^{125}I$ using the Chloramine T method [17]. Male CF-1 mice aged 6–8 weeks, weighing 22–25 g, were injected intravenously via the lateral tail vein with ^{125}I-TOC or ^{125}I-REAL-TOC, at a dose of 1×10^6 cpm per mouse, corresponding to 0.1 mg/kg of the peptide. Three to four mice were sacrificed at 10 min, 30 min, 1 h, 2 h, 4 h, 8 h and 24 h post injection. Blood samples, as well as organs of each mouse including lung, liver, spleen, intestine, kidney, pancreas and brain were collected. The radioactivity in each sample was measured using a gamma counter (Packard, Downers Grove, IL, USA).

2.6. Intrahepatic distribution

Parenchymal cells (PC) and nonparenchymal cells (NPC) constitute the major cell types in the liver. NPC consists of sinusoidal endothelial cells, Kupffer cells and hepatic stellate cells. The intrahepatic distribution of ^{125}I-TOC and ^{125}I-REAL-TOC was examined at 10 min, 1 h and 2 h post intravenous injection to mice. PC and NPC were separated following the modified two-step collagenase method [18]. Briefly, ^{125}I-TOC or ^{125}I-REAL-TOC was injected through the tail vein for the observation time points of 1 h and 2 h, and injected through the inferior vena cava for a 10-min time point after the abdomen was opened. Each mouse was anesthetized with an intraperitoneal injection of 300 μl of PBS solution containing 4.5 mg of ketamine and 0.24 mg of xylazine. At the indicated time point, the inferior vena cava was cannulated through the right atrium, the inferior vena cava below the liver was tightened, and the portal vein was opened so that the liver would be exclusively infused at a constant rate of 10 ml/min. The perfusion was started first for 3 min with oxygenated Hank's-Hepes buffer (138 mM NaCl, 5 mM KCl, 0.8 mM $MgSO_4$, 0.34 mM Na_2HPO_4, 0.44 mM KH_2PO_4, 25 mM $NaHCO_3$, 13 mM Hepes) supplemented with 0.6 mM ethylene glycol-bis(2-aminoethylether)-*N*,*N*,*N*′,*N*′-tetraacetic acid (EGTA) and 1% bovine serum albumin (BSA). The perfusion was continued for another 3 min with Hank's-Hepes buffer supplemented with 4 mM $CaCl_2$ and 0.05% collagenase IV. Following the perfusions, the liver was excised and the cells were gently scraped off by using a glass rod in 25 ml of cold Hank's-Hepes buffer containing 0.1% BSA. The crude cell suspension was filtered through a cotton mesh sieve. After sedimentation at 4 °C for 20 min, the pellet mostly contained PC ("PC pellet") and the supernatant mostly contained NPC ("NPC supernatant").

To further purify the PC pellet from NPC contamination [19], the PC pellet was washed twice with Hank's-Hepes buffer, with each wash followed by centrifugation at 50g for 1 min. The resultant purified PC pellet was suspended in 5 ml of Hank's-Hepes buffer, and cell number was counted by using hemocytometer. The NPC supernatant was centrifuged at 200g for 2 min, and the resultant NPC pellet was washed twice, suspended in Hank's-Hepes buffer, and the cell number was counted under hemocytometer.

One milliliter each of the PC and the NPC cell suspension was subjected to radioactivity measurement and the protein concentration in each suspension was measured by using the BCA assay.

2.7. Drug stability in liver slices

Fresh mouse livers were cut into small pieces of about 1 mm in width. Two grams of wet liver tissues were incubated with ^{125}I-TOC or ^{125}I-REAL-TOC in 10 ml of Dulbecco's modified Eagle's medium (DMEM) containing 5% fetal bovine serum (FBS) at 37 °C in a water bath with gentle shaking. Aliquots were taken at

0 min, 1 h, 4 h and 8 h post incubation. Size exclusion chromatography (Sephadex G25, 35 ml column, PBS/0.1% SDS buffer mobile phase) was used to fractionate the intact peptide and degradation products. The radioactivity in each 0.8-ml fraction collected was determined.

2.8. Statistical analysis

One-way ANOVA with Bonferroni adjustment was performed using SPSS 10.0 to determine the level of significance for data from animal experiments. Other data were analyzed using an independent student's *t* test, where data sets were considered to be statistically significantly different when the *p*-value was less than 0.05.

3. Results

3.1. Characterization of REAL-TOC using HPLC and MALDI-TOF analysis

REAL-TOC and TOC were analyzed by RP-HPLC under the conditions described in Section 2. The retention times of TOC and REAL-TOC were 8.10 and 15.24 min, respectively. After purification, a single peak of 15.24 min appeared in the HPLC chromatograms, indicating that the purity of REAL-TOC and TOC was over 95% in the final product (Fig. 2A). The molecular weight of REAL-TOC was determined using MALDI-TOF analysis. The measured mass $(M+H)^+$ of REAL-TOC (1752.31 Da) (Fig. 2B) is close to the calculated monoisotopic mass (1752.80 Da).

3.2. Biodistribution of ^{125}I-TOC or ^{125}I-REAL-TOC

Radioiodinated REAL-TOC and TOC were intravenously injected in mice, and the livers were excised and measured for radioactivity. ^{125}I-REAL-TOC had a significant liver accumulation with greater than 20% of the injected dose (ID)/g sustained in the liver up to 2 h post injection, and 5.8% ID/g remaining at 24 h post injection (Fig. 3). ^{125}I-TOC was quickly excreted out of the liver with only 5.33% ID/g remaining at 2 h post injection and 1.87% ID/g at 24 h post injection (Fig. 3). As a result, the area under the curve (AUC) of ^{125}I-REAL-TOC in the liver was 3.8-fold greater than that of ^{125}I-TOC.

3.3. Hepatic cellular localization of ^{125}I-TOC or ^{125}I-REAL-TOC

PC and NPC were isolated after liver perfusion following an intravenous injection of ^{125}I-REAL-TOC or ^{125}I-TOC in mice, and the drug level in each cell type was determined. At 10 min post injection, ^{125}I-REAL-TOC was distributed to both PC and NPC with a PC/NPC ratio of 0.81, while ^{125}I-TOC was dominantly distributed to PC with a PC/NPC ratio of 15.75 (Fig. 4).

The levels of ^{125}I-REAL-TOC and ^{125}I-TOC in PC were further compared at different time points post injection (Fig. 5A). ^{125}I-REAL-TOC retained in PC for up to 2 h with a relatively constant concentration (around 6% ID/100 mg protein). TOC was quickly excreted out of PC with only 2.4% ID/100 mg protein remaining at 2 h post injection. ^{125}I-REAL-TOC was also retained in NPC at a significantly higher level than ^{125}I-TOC. As shown in Fig. 5B, the ^{125}I-REAL-TOC concentration (63.1% ID/100 mg protein) was 22.5-fold higher than ^{125}I-TOC (2.8% ID/100 mg protein) at 2 h in NPC.

3.4. Drug stability in liver slices

The stability of ^{125}I-TOC and ^{125}I-REAL-TOC in mouse liver slices was measured using Sephadex G25 size exclusion chromatography. The 1st peak in the elution profile represents intact peptides remaining in the solution. As shown in Fig. 6, ^{125}I-REAL-TOC was more stable than ^{125}I-TOC in liver slices. Ninety-five percent of ^{125}I-REAL-TOC remained intact after 8-h incubation, while only 37% of ^{125}I-TOC remained intact under the same incubation conditions.

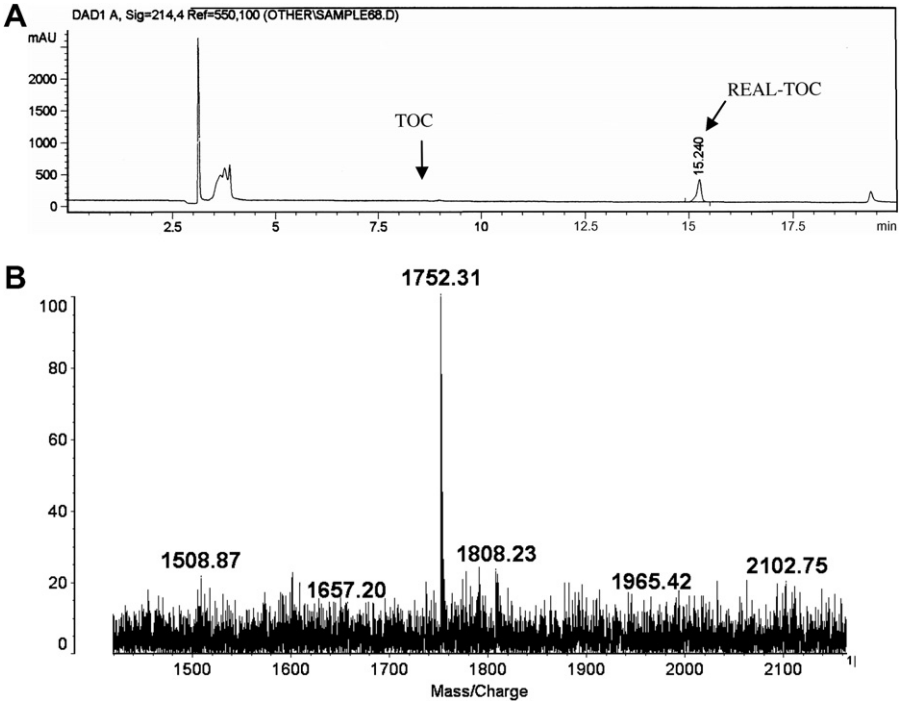

Fig. 2. Characterization of REAL-TOC. Purified REAL-TOC was analyzed by RP-HPLC chromatography (A) and MALDI-TOF (B) as described in Section 2.

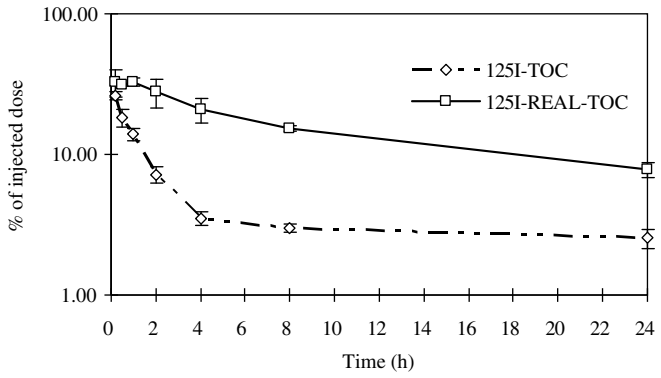

Fig. 3. Liver distribution of ^{125}I-TOC or ^{125}I-REAL-TOC. Male CF-1 mice were injected intravenously via the lateral tail vein with ^{125}I-TOC or ^{125}I-REAL-TOC, at a dose of 1×10^6 counts per minute (CPM) per mouse, corresponding to 0.1 mg/kg. Three to four mice were sacrificed each time at 10 min, 30 min, 1 h, 2 h, 4 h, 8 h and 24 h post injection. The livers were excised and the radioactivity in each sample was measured using a gamma counter. The data are expressed as the mean value of % injected dose per gram of liver tissue (% ID/g) of 3–4 animals ± standard deviation (SD).

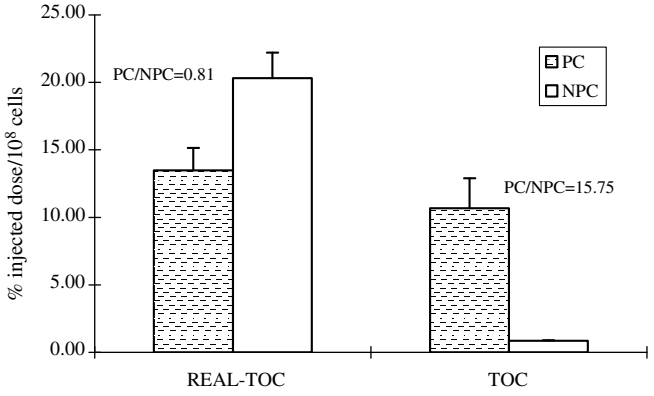

Fig. 4. Intrahepatic distribution of ^{125}I-TOC and ^{125}I-REAL-TOC. CF-1 mice were injected with ^{125}I-TOC or ^{125}I-REAL-TOC through inferior vena cava. At 10 min post injection, parenchymal cells (PC) and nonparenchymal cells (NPC) were isolated after two-step collagenase perfusion of livers. The drug level in each liver cell type was measured as % ID per 100 million cells, and the ratios of the drug concentration in PC to that in NPC (PC/NPC) were calculated.

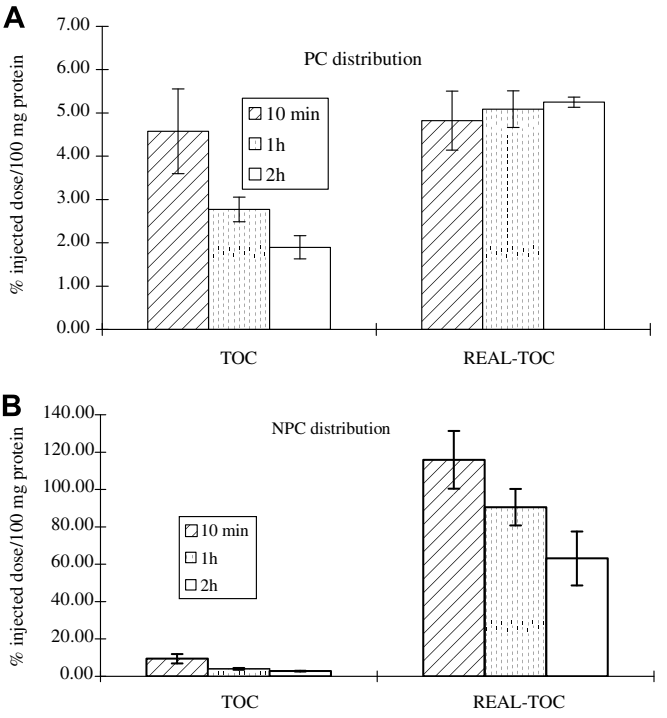

Fig. 5. The accumulation of ^{125}I-TOC and ^{125}I-REAL-TOC in parenchymal cells (A) and nonparenchymal cells (B). ^{125}I-TOC or ^{125}I-REAL-TOC was injected intravenously to mice. PC and NPC were isolated after a two-step collagenase perfusion of livers at 10 min, 1 h and 2 h following an injection. The drug concentration in each liver cell type was measured, and was expressed as means (% ID/100 mg protein) ± SE (n = 3).

4. Discussion

Somatostatin is a peptide hormone that inhibits growth hormone (GH) release through antagonizing the release of growth hormone releasing factor (GHRF). Its binding to multiple subtypes of somatostatin receptor (SSR1-5) also elicits the inhibition of cell proliferation in many tumors [20,21]. In addition, other anti-tumor mechanisms include indirect inhibition of insulin-like growth factor-1 (IGF-1) through down-regulation of GH release and direct inhibition of tumor angiogenesis [22–24]. Therefore, somatostatin analogues such as octreotide have been implicated in the chemotherapy of lung cancer [25], breast cancer [26] and recently hepatocellular carcinoma (HCC) [27–29]. However, octreotide has presented controversial therapeutic benefits in patients with HCC. Some clinical trials have demonstrated the improving survival benefits in patients [27–29], while other clinical trials failed [12,30]. We reason that targeting of somatostatin analogues to the liver might improve their chemotherapeutic effect in HCC through intensifying the doses in the liver cells.

In this study, we prepared a reversibly lipidized derivative of TOC, REAL-TOC, by conjugating two palmitoyl cysteinyl residues to a TOC molecule through disulfide linkages. TOC could be regenerated upon the reduction of the disulfide bonds *in vivo*. When intravenously administered to mice, REAL-TOC was slowly cleared from the blood, resulting in an extended elimination half-life, which is consistent with the prolonged biological effect of lipidized octreotide as described in our previous report [10]. More importantly, this conjugation exhibited an increased hepatic uptake, and a sustained liver accumulation for up to 24 h. Within the liver, both parenchymal and nonparenchymal cells contribute to the enhanced uptake of REAL-TOC, with the concentration of parenchymal cell-associated REAL-TOC remaining constant for more than 2 h. While REAL-TOC was gradually eliminated from nonparenchymal cells, the level of the lipidized peptide was still 22.5-fold higher than that of TOC at 2 h post injection. This observed increase in liver cell uptake and retention may be due to the increased hydrophobicity and nonspecific binding of the lipidized derivative to plasma proteins, such as lipoproteins and albumin. Kupffer cells and sinusoidal endothelial cells are first encountered by TOC or REAL-TOC in the liver before hepatocytes are accessible. These cells phagocytose large lipophilic molecules such as liposome or albumin-bound lipophilic drugs through scavenger receptors [31]. Therefore, the phagocytosis by Kupffer cells and sinusoidal endothelial cells may account for the initially high uptake of REAL-TOC in nonparenchymal cells.

Reversible lipidization presents a novel liver-targeting approach. Different from mannosylation and galactosylation approaches that have been widely used to modify drugs for targeting liver, the lipids conjugated to TOC enhance the association of TOC with liver cells, while not necessarily triggering the internalization. Additionally, reversible lipidization not only increases the absorption of peptide drugs in both types of liver cells, but also prolongs the plasma half-life of peptide drugs. The disulfide bonds that were introduced in the conjugation allow the release of native peptides upon reduction *in vivo*, as previously demonstrated in lipidized desmopressin [32]. There are several possible sites for the reduction of the disul-

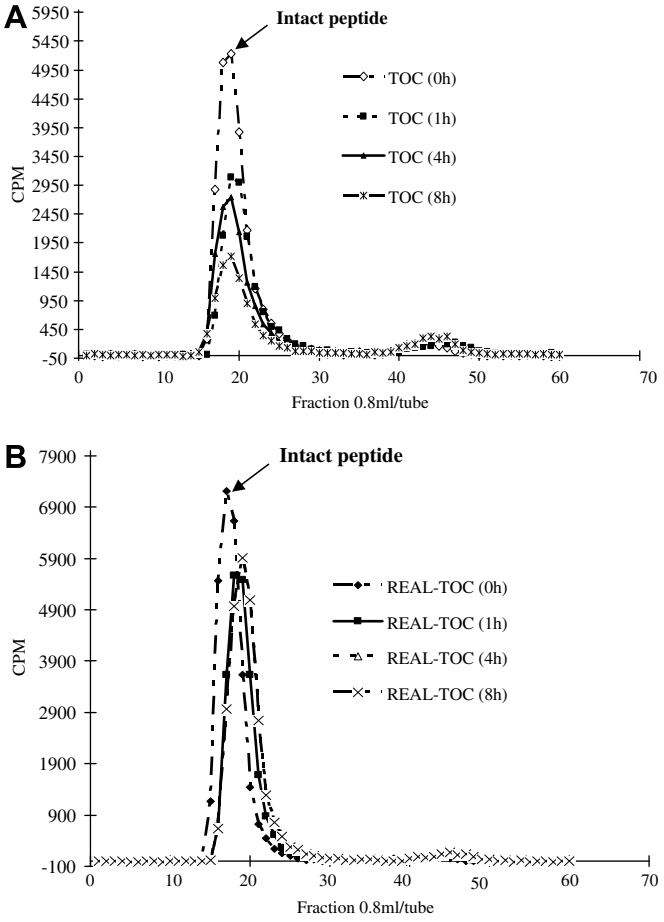

Fig. 6. The metabolic stability of ^{125}I-TOC (A) and ^{125}I-REAL-TOC (B) in mouse liver slices. The compounds were incubated in liver slices at 37 °C at the indicated time points of 0, 1, 4 and 8 h. The samples were analyzed for degradation using a Sephadex G25 size exclusion chromatography gel. Fraction volumes of 0.8 ml were collected and the radioactivity was determined and presented as CPM.

fide linkages. For example, the reduction could be facilitated on the liver cell surface as sinusoidal efflux of reduced glutathione (GSH) in hepatocytes [33] possibly creates a reductive state on the cell surface, together with cell membrane-associated protein disulfide isomerase (PDI) [34]. The disulfide linkage may also be reduced inside cells upon absorption. The intracellular GSH/GSSG ratio is around 100, and thioredoxin family enzymes act as catalytic effectors to facilitate reduction [35]. In any case, upon the reduction, the native peptide will be regenerated from the lipidized peptides to exert a therapeutic function.

Our data indicate that reversible lipidization carries several potential advantages for improving the therapeutic efficacy of somatostatin analogues in HCC. First, the lipidized peptide exerted a protracted biological activity which we had previously reported [10]; secondly, the lipidized peptide has a prolonged plasma half-life; thirdly and most importantly, the dose regime of REAL-TOC has been intensified in the liver with a sustained high association with both parenchymal cells and nonparenchymal cells. All these improved properties of TOC brought by reversible lipidization would enhance the drug exposure to the liver while increasing patient compliance by allowing the reduction of dosage and dosing frequency. The sustained high association of REAL-TOC with parenchymal cells and nonparenchymal cells might enhance the anti-tumor effect in the liver, which is especially beneficial for the patients with HCC who are not responsive to somatostatin therapy.

In conclusion, besides the improvement of the pharmacokinetics and stability, reversible lipidization can significantly increases the delivery of somatostatin analogues to the liver. Therefore, this lipid-based approach provides a novel passive liver targeting strategy for peptide and protein drugs.

Acknowledgements

The authors acknowledge Daisy Shen for the excellent technical support and Jennica Zaro, Ph.D. for the proofreading of the manuscript. This work was supported in part by a contract from Pharmdel, Inc. (San Jose, CA, USA).

References

[1] L. Fiume, C. Busi, A. Mattioli, Targeting of antiviral drugs by coupling with protein carriers, FEBS Lett. 153 (1983) 6–10.
[2] L. Fiume, C. Busi, G. Di Stefano, A. Mattioli, M. Torrani-Cerenzia, F. Bonino, G. Capra, W. De Bernardi, A. Ponzetto, B. Lavezzo, et al., Liver targeting of adenine arabinoside monophosphate (ara-AMP) by coupling to lactosaminated human serum albumin, Ital. J. Gastroenterol. 27 (1995) 189–192.
[3] L. Beljaars, D.K. Meijer, K. Poelstra, Targeting hepatic stellate cells for cell-specific treatment of liver fibrosis, Front. Biosci. 7 (2002) e214–e222.
[4] H. Sato, Y. Kato, E. Hayasi, T. Tabata, M. Suzuki, Y. Takahara, Y. Sugiyama, A novel hepatic-targeting system for therapeutic cytokines that delivers to the hepatic asialoglycoprotein receptor, but avoids receptor-mediated endocytosis, Pharm. Res. 19 (2002) 1736–1744.
[5] S.W. Lamberts, A.J. van der Lely, W.W. de Herder, L.J. Hofland, Octreotide, N. Engl. J. Med. 334 (1996) 246–254.
[6] C.E. Samuel, Antiviral actions of interferons, Clin. Microbiol. Rev. 14 (2001) 778–809. table of contents.
[7] J.H. Hoofnagle, L.B. Seeff, Peginterferon and ribavirin for chronic hepatitis C,N. Engl. J. Med. 355 (2006) 2444–2451.
[8] J. Wang, D. Chow, H. Heiati, W.C. Shen, Reversible lipidization for the oral delivery of salmon calcitonin, J Control. Release 88 (2003) 369–380.
[9] J. Wang, D. Wu, W.C. Shen, Structure–activity relationship of reversibly lipidized peptides: studies of fatty acid-desmopressin conjugates, Pharm. Res. 19 (2002) 609–614.
[10] L. Yuan, J. Wang, W.C. Shen, Reversible lipidization prolongs the pharmacological effect, plasma duration, and liver retention of octreotide, Pharm. Res. 22 (2005) 220–227.
[11] G. Treiber, C. Rocken, T. Wex, P. Malfertheiner, Octreotide alone or in combination with rofecoxib as palliative treatment for advanced hepatocellular cancer, Z. Gastroenterol. 45 (2007) 369–377.
[12] G. Becker, H.P. Allgaier, M. Olschewski, A. Zahringer, H.E. Blum, Long-acting octreotide versus placebo for treatment of advanced HCC: a randomized controlled double-blind study, Hepatology (Baltimore, MD) 45 (2007) 9–15.
[13] W.A. Slijkhuis, L. Stadheim, Z.M. Hassoun, U.C. Nzeako, W.K. Kremers, J.A. Talwalkar, G.J. Gores, Octreotide therapy for advanced hepatocellular carcinoma, J. Clin. Gastroenterol. 39 (2005) 333–338.
[14] C. Lersch, R. Schmelz, J. Erdmann, R. Hollweck, E. Schulte-Frohlinde, F. Eckel, M. Nader, V. Schusdziarra, Treatment of HCC with pravastatin, octreotide, or gemcitabine – a critical evaluation, Hepatogastroenterology 51 (2004) 1099–1103.
[15] J.T. Siveke, C. Herberhold, C. Folwaczny, Complete regression of advanced HCC with long acting octreotide, Gut 52 (2003) 1531.
[16] G. Weckbecker, F. Raulf, B. Stolz, C. Bruns, Somatostatin analogs for diagnosis and treatment of cancer, Pharmacol. Ther. 60 (1993) 245–264.
[17] P.J. McConahey, F.J. Dixon, Radioiodination of proteins by the use of the chloramine-T method, Methods Enzymol. 70 (1980) 210–213.
[18] P. Moldeus, J. Hogberg, S. Orrenius, Isolation and use of liver cells, Methods Enzymol. 52 (1978) 60–71.
[19] C. Managit, S. Kawakami, M. Nishikawa, F. Yamashita, M. Hashida, Targeted and sustained drug delivery using PEGylated galactosylated liposomes, Int. J. Pharm. 266 (2003) 77–84.
[20] G. Weckbecker, L. Tolcsvai, B. Stolz, M. Pollak, C. Bruns, Somatostatin analogue octreotide enhances the antineoplastic effects of tamoxifen and ovariectomy on 7,12-dimethylbenz(alpha)anthracene-induced rat mammary carcinomas, Cancer Res. 54 (1994) 6334–6337.
[21] C. Bruns, G. Weckbecker, F. Raulf, K. Kaupmann, P. Schoeffter, D. Hoyer, H. Lubbert, Molecular pharmacology of somatostatin-receptor subtypes, Ann. N. Y. Acad. Sci. 733 (1994) 138–146.
[22] E.A. Kouroumalis, Octreotide for cancer of the liver and biliary tree, Chemotherapy 47 (Suppl. 2) (2001) 150–161.
[23] C. Scarpignato, I. Pelosini, Somatostatin analogs for cancer treatment and diagnosis: an overview, Chemotherapy 47 (Suppl. 2) (2001) 1–29.
[24] C. Bousquet, E. Puente, L. Buscail, N. Vaysse, C. Susini, Antiproliferative effect of somatostatin and analogs, Chemotherapy 47 (Suppl. 2) (2001) 30–39.
[25] K.J. O'Byrne, A.V. Schally, A. Thomas, D.N. Carney, W.P. Steward, Somatostatin, its receptors and analogs, in lung cancer, Chemotherapy 47 (Suppl. 2) (2001) 78–108.
[26] M. Pollak, The potential role of somatostatin analogues in breast cancer treatment, Yale J. Biol. Med. 70 (1997) 535–539.

[27] D.N. Samonakis, J. Moschandreas, T. Arnaoutis, P. Skordilis, C. Leontidis, I. Vafiades, E. Kouroumalis, Treatment of hepatocellular carcinoma with long acting somatostatin analogues, Oncol. Rep. 9 (2002) 903–907.
[28] M. Raderer, M.H. Hejna, C. Muller, G.V. Kornek, A. Kurtaran, I. Virgolini, W. Fiebieger, G. Hamilton, W. Scheithauer, Treatment of hepatocellular cancer with the long acting somatostatin analog lanreotide in vitro and in vivo, Int. J. Oncol. 16 (2000) 1197–1201.
[29] J.T. Siveke, C. Folwaczny, C. Herberhold, Complete regression of advanced HCC with long acting octreotide, Gut 52 (2003) 1531.
[30] J. Cebon, Somatostatin receptor expression, tumour response, and quality of life in patients with advanced hepatocellular carcinoma treated with long-acting octreotide, Br. J. Cancer 95 (2006) 853–861.
[31] J.A. Kamps, H.W. Morselt, P.J. Swart, D.K. Meijer, G.L. Scherphof, Massive targeting of liposomes, surface-modified with anionized albumins, to hepatic endothelial cells, Proc. Natl. Acad. Sci. USA 94 (1997) 11681–11685.
[32] J. Wang, D. Shen, W.C. Shen, Preparation, purification, and characterization of a reversibly lipidized desmopressin with potentiated anti-diuretic activity, Pharm. Res. 16 (1999) 1674–1679.
[33] L.D. DeLeve, N. Kaplowitz, Glutathione metabolism and its role in hepatotoxicity, Pharm. Ther. 52 (1991) 287–305.
[34] K. Terada, P. Manchikalapudi, R. Noiva, H.O. Jauregui, R.J. Stockert, M.L. Schilsky, Secretion, surface localization, turnover, and steady state expression of protein disulfide isomerase in rat hepatocytes, J. Biol. Chem. 270 (1995) 20410–20416.
[35] G. Saito, J.A. Swanson, K.D. Lee, Drug delivery strategy utilizing conjugation via reversible disulfide linkages: role and site of cellular reducing activities, Adv. Drug Deliv. Rev. 55 (2003) 199–215.